

# Two Types of Gradual Events: Solar Protons and Relativistic Electrons

A. B. Struminsky<sup>a,\*</sup>, Yu. I. Logachev<sup>b</sup>, I. Yu. Grigorieva<sup>c</sup>, and A. M. Sadovskii<sup>a</sup>

<sup>a</sup>*Space Research Institute, Russian Academy of Sciences, Moscow, Russia*

<sup>b</sup>*Institute of Nuclear Physics, Moscow State University, Moscow, Russia*

<sup>c</sup>*Central Astronomical Observatory at Pulkovo, Russian Academy of Sciences, St. Petersburg, Russia*

\**e-mail: astrum@iki.rssi.ru*

Received March 9, 2020; revised May 6, 2020; accepted May 29, 2020

**Abstract**—The gradual solar flares on April 21, 2002 (X1.5), and August 24, 2002 (X3.1), played an important role in the formation of the modern paradigm of acceleration of solar energetic particles (SEPs), according to which the difference in the observed composition of SEP ions is due to acceleration on a quasi-parallel (event of April 1–21) or quasi-perpendicular (event of August 2–24) shock wave. In our opinion, ions were accelerated not by shock waves but directly in parent flares, and it was the flare properties, in this case, their impulsive phases, that differed. Flare 1 had an unpronounced, impulsive phase, while Flare 2 had a pronounced impulse phase when the maximum intensity of microwave ( $\mu$ ) radiation was about an order of magnitude greater than that in Flare 1. Flare 2 experienced a rapid heating of plasma and an increase in the emission measure due to chromospheric evaporation, which can change the ion composition in the acceleration region. Simultaneous increases in the fluxes of relativistic electrons and protons with similar time profiles were observed in the interplanetary space (IS) after flares 1 and 2. However, there was an increase in the flux of relativistic electrons not accompanied by protons in the IS for the first 20 min only after Flare 2. These observational facts make it possible to introduce the gradual stochastic acceleration into the scenario of the considered events. In it, charged particles are accelerated in a set of elementary events that are shorter in duration than the full duration of the acceleration process.

**Keywords:** solar flares, X-ray and radio emission, coronal mass ejection, acceleration of solar protons and electrons, solar electron and proton events

**DOI:** 10.1134/S001679322008023X

## 1. INTRODUCTION

According to Benz (2017), a solar flare is an increase in the intensity of electromagnetic radiation (EMR) that has a duration of several minutes to several hours. The flare is conditionally divided into pre-flare, impulse, and explosive phases. The impulsive phase is usually defined as the processes from the onset of hard X-ray (HXR-) and  $\mu$  radiation to the maximum soft X-ray (SXR-) radiation. The explosive phase is characterized by a Doppler shift of optical lines and lasts up to the  $H_{\alpha}$  radiation maximum. A decrease phase of SXR and  $H_{\alpha}$  radiation intensity ends the flare. A post-eruptive phase, which contains the explosive phase and the decay phase, is singled out in gradual flares accompanied by eruption of matter.

The ability to accelerate charged particles up to relativistic energies is the most important property of solar-flare plasma. It is the energetic particles that interact with the matter of the solar atmosphere, and its magnetic fields generate non-thermal X-ray, radio, and  $\gamma$ -radiation that serve as a diagnostic tool for solar

flares (Benz, 2017; Ramaty et al., 1978; Miller et al., 1997; and references there). Solar energetic particles (SEPs) can also be observed in interplanetary space (IS). However, we do not know exactly which physical mechanism is responsible for the acceleration of particles interacting in the Sun and/or propagating in the IS.

The results of observations indicate that there are two phases (mechanisms) of acceleration (Wild et al., 1963, Ramaty et al., 1978; Shih et al., 2009) in solar flares. In the first phase, electrons with energies  $<300$  keV are accelerated, while electrons  $>300$  keV and protons are accelerated in proportional quantities in the second phase. It is common to associate the “first” acceleration phase with the flare impulsive phase and the “second” acceleration phase with the post-eruptive flare phase. There is a view, the so-called “modern paradigm” (Cliver, 2009; Cliver, 2019; and references there), in which electrons are accelerated in the first and second phases of the flare and protons are accelerated in the coronal mass ejection (CME) shock front.

**Table 1.** Mechanisms of acceleration considered by Miller et al. (1997) and the possibility of electron and proton acceleration in them

Observations	Sub-Dreicer E	Super-Dreicer E	MHD Turbulence	Shocks
~100-keV electrons	Yes	Yes	Yes	Yes
~10-MeV electrons	No	?	Yes	?
~100-MeV protons	No	?	Yes	Yes

In debates on the origin of solar protons, proponents of flares argue that there is a good correlation between the intensity (fluences) of EMR flares (Chertok, 2018; Belov et al., 2007; Grechnev et al., 2015, 2017) and proton fluxes (fluences) in the IS. Shock wave advocates place the emphasis on proton events, which do not fit into the found patterns and are characterized by relatively weak EMR flare fluxes (Cliver, 2016; Gopalswamy et al., 2015; Cliver et al., 2019). A series of works (see Daibog et al., 1993 and references there) considered flares with a weak impulsive phase according to  $\mu$  radiation data but with powerful solar proton fluxes in the IS. In particular, it was shown that the abnormal relationship between electrons and protons can be explained by the characteristics of flare loops.

The ability to accelerate electrons to ~10 MeV and protons to ~100 MeV is critical in the selection of an acceleration mechanism. Table 1 shows different mechanisms of acceleration and ideas on the possible acceleration of electrons and protons to a given energy, which was considered by Miller et al. (1997). Any of the four acceleration mechanisms (Table 1) can work in the first phase, but only the last two can work in the second. Information on 10-MeV electrons can be obtained from the modeling of results of observations in the radio, X-ray, and  $\gamma$ -bands, but there is currently no unequivocal solution to this problem. In principle, it is impossible to obtain information on protons interacting in the Sun with energies of 30–300 MeV (between the proton energies sufficient to generate nuclear  $\gamma$  lines and  $\pi^0$  mesons).

It was proposed (Struminsky et al., 2020) that the time profiles of solar electron fluxes of ~10 MeV and protons of >100 MeV in the IS immediately after solar flares be compared for the selection of the acceleration mechanism. It was possible to separate the electrons and protons accelerated in the first and second phases of flares near the Earth in the study of SEP events in September 2017 and their parent flares (Struminsky et al., 2020). It was assumed that a stochastic acceleration mechanism, in which protons and electrons acquire energy in many elementary acts that are much shorter than the flare itself, was implemented (Benz, 1985; Lu and Hamilton, 1991; Vlahos et al., 1989).

It seems necessary to take into account gyrosynchrotron losses of electrons to radiation in the second phase (Svestka, 1970), which can be neglected in the first phase, to reconcile the stochastic acceleration

process with the observation of two phases of acceleration in solar flares (Wild et al., 1963; Ramaty et al., 1978; Shih et al., 2009). In this case, the first and second phases of acceleration differ only in that the energy of accelerated protons is small for their detection on the Sun in the first phase, but it can reach values sufficient for the generation of nuclear  $\gamma$ -lines and  $\pi$ -mesons in the second phase.

A CME is necessary to implement the second acceleration phase. Its role is (1) to attract more and more loops into the flare process in the height range from the chromosphere to the corona, (2) to bring the energetic particles back to the flare region, (3) to additionally accelerate the particles on the shock front of the CME, and (4) to provide them with the conditions for escape to the IS. The latest results of magnetohydrodynamic modeling (Masson et al., 2019) show that episodes of multiple magnetic reconnection occur both before and after the CME. In addition to the reconnection episodes that form a rope, there are reconnection episodes between closed corona field lines and open IS field lines that allow the escape of accelerated particles in the flare, as confirmed by observations (Grechnev et al., 2017; Kocharov et al. 2017).

It is of interest to test the proposed scenario on significant proton events and their parent flares. For this purpose, we chose for the present work the gradual solar flares on April 21, 2002 (X1.5), and August 24, 2002, (X3.1), and studied related SEP events. The ion composition in the first event was coronal at high energies and chromospheric in the second (Tylka et al., 2005, 2006). According to the interpretation in these articles, ions were accelerated by shock waves, and the difference in the observed ion composition was due to acceleration at quasi-parallel (Event 1) or quasi-perpendicular shock waves (Event 2) of the CME. In our opinion, Tylka et al. (2005, 2006) did not take into account the difference in the parent flares and did not consider the properties of solar relativistic electron fluxes in the IS.

The purpose of this article is to show the difference between the two flares based on observations in the SXR- and radio emission and to introduce the notion of two classes of proton flares with powerful and weak EMR fluxes, i.e., with pronounced and nonpronounced impulsive phases, on their example in order to show that the SEP events observed after these flares differed not only in ion composition but also in time profiles of relativistic solar electrons. An accounting

for these factors leads us to the conclusion that the ions in SEP-events were mainly accelerated in post-eruptive phase flares, and it is the differences between the flares that are important, not those between the shock waves.

## 2. OBSERVATIONAL METHODS AND DATA

Here, we compare the fluxes of relativistic electrons (SOHO/EPHIN) with proton fluxes of  $>100$  MeV (GOES) and neutron-monitor (NM) counting rates in order to study the properties of particle populations accelerated in the first and second phases of solar flares.

We introduce the starting point, the zero time, in order to compare different events in one time scale. Since phases (acceleration mechanisms) differ in the presence or absence of relativistic electrons (Ramaty et al., 1978; Shih et al., 2009), we take the beginning of the detection of  $\mu$ -radiation at 15.4 GHz (Table 1, data from the Radio Solar Telescope Network, RSTN), which is generated by relativistic electrons in the solar magnetic field, as the zero time in each considered event, as in an earlier work (Struminsky et al., 2020). The selected zero time can be considered as the time of appearance of relativistic electrons in the atmosphere of the Sun and as a conventional boundary between the first and second phases. Since the selected events do not contain data on  $\gamma$ -lines, we further specify the boundary between the acceleration phases by the observation of solar protons in the orbit of the Earth and estimate the time of their earliest escape to the IS.

Currently, the only detector of relativistic electrons in Earth's orbit is the Electron Proton Helium Instrument (EPHIN) (Müller-Mellin et al., 1995) onboard the Solar and Heliospheric Observatory (SOHO), which is at Lagrangian point L1. Data on relativistic electron fluxes in channels 0.27–0.7, 0.67–3.0, and 2.64–6.12 MeV is publicly available at <http://www2.physik.uni-kiel.de/SOHO/phpeph/EPHIN.htm>. The ratio of the speed of electrons to the speed of light  $V/c$  is within 0.78–0.91, 0.91–0.99, and 0.99, respectively. If the length of the field line along which the particles propagate is minimal (i.e.  $\sim 1.2$  au), the electrons in the differential channels will be delayed relative to the electromagnetic radiation by  $\sim 4$ , 3, and 2 min. The data of the GOES integral proton channels are available at [https://cdaw.gsfc.nasa.gov/CME\\_list/NOAA/particle/](https://cdaw.gsfc.nasa.gov/CME_list/NOAA/particle/). For protons at energies 10, 100, and 500 MeV ( $V/c = 0.15$ , 0.43, and 0.76), the delay will be  $\sim 58$ , 15, and 5 min.

We successively used two data bases to select the NM, which showed the fastest ground level enhancement (GLE) of cosmic ray intensity. The GLE event database of the University of Oulu (<http://cosmicrays oulu.fi/GLE.html>) makes it possible to select seven NMs that showed the best time profiles from the 5-min data. We then compared the 1-min data from

these seven selected NMs, which are available at <http://www.nmdb.eu/nest/search.php>, and selected the NM that showed the fastest GLE beginning. In the case of the GLE event of August 24, 2002, it was NM SOPO (South Pole) with a zero geomagnetic cutoff threshold, i.e., we detected protons with energies  $>500$  MeV.

Information on the events was taken from the *solar events* files from <ftp://ftp.swpc.noaa.gov/pub/indices/events/>, and information on CMEs was taken from [https://cdaw.gsfc.nasa.gov/CME\\_list/](https://cdaw.gsfc.nasa.gov/CME_list/). We also used 3-s data from two standard GOES SXR channels (1–8 Å and 0.5–4 Å) from [satdat.ngdc.noaa.gov/sem/goes/data/](http://satdat.ngdc.noaa.gov/sem/goes/data/) to calculate the emission measures ( $EM$ ) and temperature ( $T$ ) of the flare plasma in *Solar-Soft*. The solar radio data were taken from the public domain (RSTN, <ftp.ngdc.noaa.gov/STP/space-weather/solar-data/solar-features/solar-radio/>).

## 3. ANALYSIS OF OBSERVATIONS

Table 2 presents the characteristics of the considered events. According to the definition by Benz (2017), the impulsive phase lasted 47 min in Flare 1 and 19 min in Flare 2. Since we estimate that the CME occurred before the radio burst of type II, before (+10) min on our scale (Table 2), electron acceleration, which was accompanied by HXR and  $\mu$  bursts, continued during the post-eruptive phase in both flares. The synchronicity of the acceleration of the CME with hard X-ray bursts established earlier for a number of eruptive flares (e.g., Zhang et al. 2001; Temmer et al. 2010) does not apply to the post-eruptive phase.

Note that the SXR maximum in these flares was determined by the  $EM$  maximum and not the  $T$  maximum (Figs. 1a and 2b, Table 2). The flares differed both in their maximum  $T$  and  $EM$  values and their rate of increase (Figs. 1a and 1b). These parameters were significantly lower in Flare 1 than in Flare 2, which seems to be due to the difference between nonthermal processes in the preflare and impulsive phases. In Flare 1,  $T$  and  $EM$  increased slowly and persistently from the beginning of the preflare phase to their maxima in the impulsive phase, and several maxima caused by individual heating episodes (acceleration of nonthermal electrons) can be seen in the  $T$  graph.

According to the data on SXR and radio emissions in both flares (see Fig. 1), the accelerated electrons interacted with the solar matter simultaneously within a large altitude range from the chromosphere to the corona during the impulsive phase. The maximum intensity of  $\mu$ -radiation (15.4 GHz) in Flare 2 was an order of magnitude higher than that in Flare 1 with a comparable coronal plasma radiation intensity at (245 MHz) in both flares.

High intensities of  $\mu$ -radiation correspond to a greater number of electrons in strong magnetic fields, i.e., they are closer to the source of the main energy

**Table 2.** Some characteristics of the considered events relative to the selected zero time in minutes

Date, zero time, flare class and coordinates	Apr 21, 2002, <b>0108 UT</b> X1.5 S14W84	Aug. 24, 2002 <b>0053 UT</b> X3.1 S02W81
Start and maximum of the SXR Flare (GOES)	−25 min/+47 min	−4 min/+19 min
Time $T_{\max}$ /delays of $EM_{\max}$ relative to $T_{\max}$	+25 min/22 min	+9 min/10 min
Time of appearance of the CME (LASCO_C2) and its speed	+19 min 2393 km/s	+34 min 1913 km/s
Lowest radio frequency detected by RSTN, start and maximum	245 MHz +3 min/+3 min +35 min/+81 min	245 MHz +8 min/+9 min
Maximum radiation at 15.4 GHz	+15 min 1300 sfu	+7 min 17000 sfu
Beginning times of bursts of types III, II, and IV	+9 min/+11 min/+40 min	+7 min/+16 min/+22 min
Time of the beginning of the increase of smoothed average >100-MeV proton fluxes (GOES) and 2.64- to 6.12-MeV electrons (SOHO/EPHIN) from the first and second acceleration phases	+27 min/no data/+25 min	+22 min/+5/+28 min

release of the flare, which is traditionally associated with the impulsive phase (Benz, 2017; Grechnev et al., 2015). Obviously, large magnetic fields in the flare region are located deeper in the Sun's atmosphere. Therefore, the beam of accelerated electrons was focused on a plasma target of smaller area but higher density. In this case, strong local plasma heating and effective chromospheric evaporation, i.e., large HXR and SXR fluxes, are expected. This is why we believe that the impulsive phase was expressed more strongly in Flare 2 than in Flare 1.

In the decay phase, the calculated  $T$  of plasma was approximately the same in Flares 1 and 2 (Fig. 1a), but the  $EM$  (Fig. 1b) and radio flux (Fig. 1c) in Flare 1 were larger after (+50) min. Therefore, the nonthermal processes in Flare 1 after (+50) min were stronger, and they developed in a larger volume of plasma.

Flare 1 was the first large flare observed by RHESSI after it was placed into orbit. The results were analyzed by Gallagher et al. (2002). The HXR maximum probably occurred during the SC night and was missed. The HXR time profiles showed many peaks against the background of a smooth increase in intensity before the night and decay after the SC night. Flare 2 did not occur during the RHESSI observation time, and we have no information about its HXR emission.

Since there are no data on nuclear  $\gamma$ -lines in these events, let us turn to observations of solar electrons and protons in IS in order to specify the beginning of the second acceleration phase and its duration. Figure 2 compares the time profiles of the fluxes of (a) protons and (b) electrons for two events in the same time scales and particle fluxes.

The proton flux in Event 1 began to increase with a delay (light squares, Fig. 2a) and continued to increase

continuously to (+120) min. In Event 2, there was an earlier arrival of protons (black squares, Fig. 2a). Their intensity increased rapidly until the beginning of the plateau by  $\sim$ (+60) min and remained higher until (+120) min (Fig. 2a). The electron fluxes in Event 1 began to increase by (+25) min (light circles, Fig. 2b). In Event 2, the arrival of the first electrons was detected at (+5) min, and the second increase of their intensity began at (+28) min (black circles, Fig. 2b). The electron fluxes in Events 1 and 2 were comparable from (+28) to (+40) min, but the electron fluxes of Event 1 then became larger (Fig. 2b). This behavior of electron and proton fluxes in Event 1 is associated with increased activity in the corona after (+40) min (Fig. 1b).

In Event 1, the flux increase occurred at (+25) min for electrons and at (+27) min for protons (Fig. 3a and Table 2), while it was at (+28) and (+22) min in Event 2 (Fig. 3b, Table 2), respectively. The large time difference between the arrival of protons and electrons in Event 2 is associated with the fact that only the intensity of relativistic electrons increased from (+5) to (+22) min. Note that Kocharov et al. (2020) did not trust the EPHIN detector during a similar increase in the event of September 10, 2017, believing that it can add X-ray photons in the impulsive flare phase. In our opinion, if there is such an effect, it is insignificant and does not affect the results of our phenomenological analysis. Recall that RHESSI did not observe Flare 2, which makes it impossible to compare HXR fluxes in Flares 1 and 2 to test the assumption of Kocharov et al. (2020).

In Event 2, the first electrons in the 2.64- to 6.12-MeV channel ( $\alpha = v/c = 0.99$ ) were detected by SOHO/EPHIN at (+5) min. If they exited at the zero time, they traveled  $s = 1.62$  au. If protons traveled the same path as electrons, their delay time for an energy

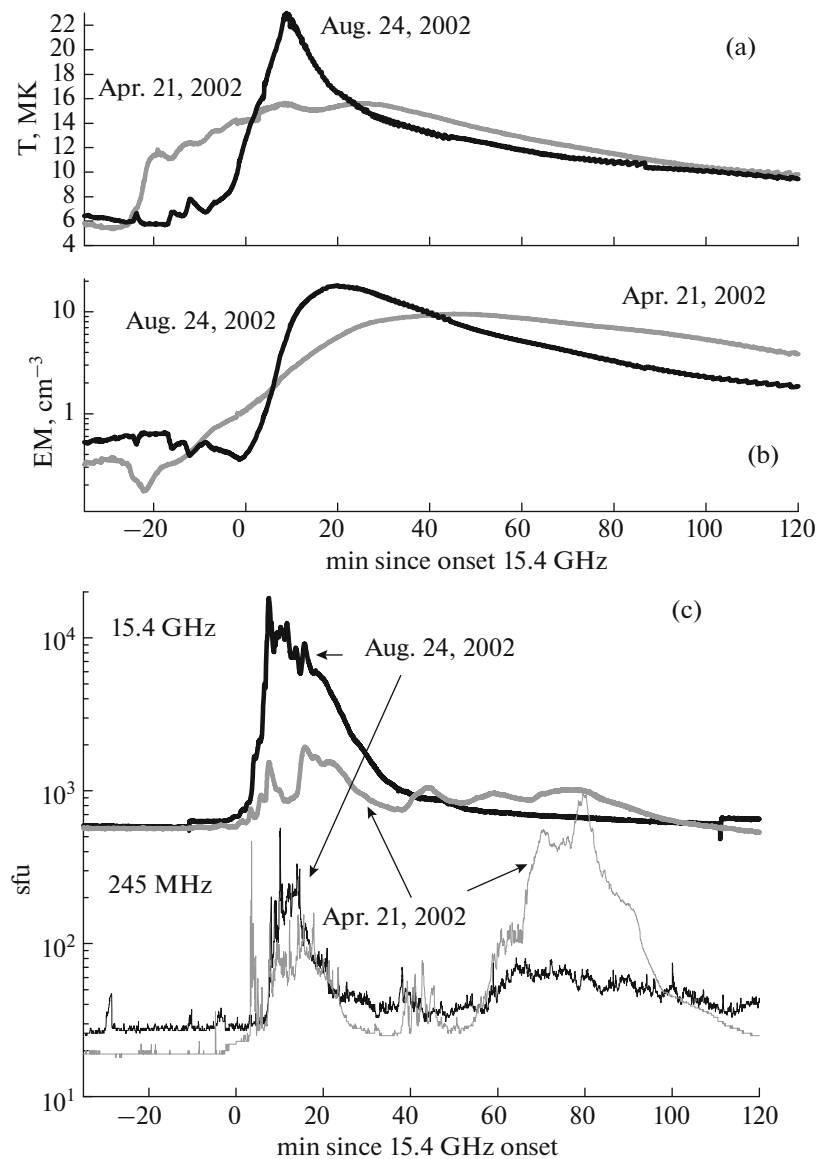


**Fig. 1.** Time profiles of the (a) temperature and (b) emission measure of flare plasma in the approximation of one temperature; (c) radio emission intensities at frequencies of 245 MHz and 15.4 GHz (RSTN) in the flares of Apr. 21, 2002 (gray lines), and Aug. 24, 2002 (black lines).

of 100 MeV ( $\alpha = v/c = 0.43$ ) relative to electromagnetic radiation (EMR) is  $\sim 23$  min. The expected time of 100-MeV protons escaping to the IS is  $-(-1)$  min, which agrees quite well with the boundary between the first and second phases of acceleration and the estimate of the time of the CME position on one solar radius. Protons at 500 MeV ( $\alpha = 0.76$ ), to which polar NMs are sensitive, should lag behind the EMR by  $\sim 10$  min. In the case of the same propagation length and the beginning of the GLE event at 0117 UT  $\pm 3$  min (Tylka et al., 2006), (i.e., at  $(+24) \pm 3$  min relative to 0 in our scale), the expected time for GLE protons to escape to the IS from the Sun is at 0100 UT  $((+24) - 10 \pm 3 = (+14) \pm 3$  min, relative to 0), i.e., obviously later than 100-MeV protons.

Figure 4 compares the count rate variation of South Pole NM in the GLE event of August 21, 2002, with the integral proton flux of  $>100$  MeV (Fig. 4a) and with the differential electron flux in the 2.64- to 6.12-MeV channel (Fig. 4b). The NM count rate variations start to increase later and to decrease earlier than the  $>100$ -MeV proton flux (Fig. 4a) and the electron flux in the 2.64- to 6.12-MeV channel (Fig. 4b). In particular, this could take place if injections of  $>100$ -MeV protons and 2.64- to 6.12-MeV electrons began earlier and ended later than the injection of the  $>500$ -MeV proton flux. The acceleration and escape of  $>500$ -MeV protons to the IS lasted about 30 min, and the escape of

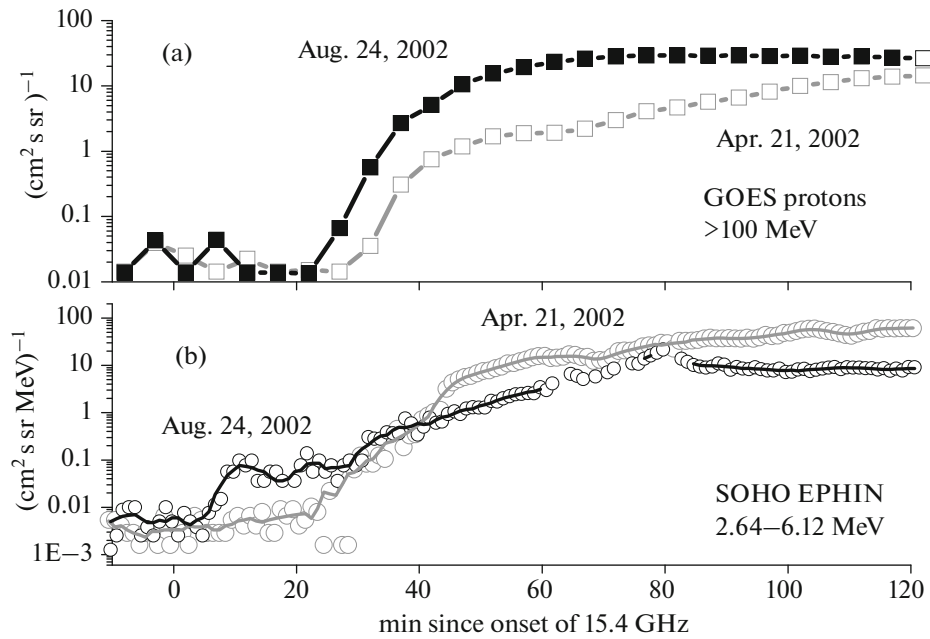


**Fig. 2.** Time profiles of fluxes of (a)  $>100$ -MeV protons (GOES) and (b) 2.64- to 6.12-MeV electrons (SOHO EPHIN) detected in the events of Apr. 21, 2002 (gray icons) and Aug. 24, 2002 (black icons).

$>100$ -MeV protons and 2.64- to 6.12-MeV electrons lasted more than 100 min.

In Event 1 we cannot estimate the length of the field line along which the particles propagated by the arrival time of electrons from the first acceleration phase. The delay in the beginning of the increase in  $>100$ -MeV protons in Event 1, relative to Event 2, can be caused by both the longer length of the field line and the later acceleration and escape of  $>100$ -MeV protons to the IS. The argument in favor of the latter variant is that, according to the linear approximation of the LASCO-C2 data (Figs. 3a–3b), the CME in Event 1 was delayed by about 10 min relative to the selected zero time, and it almost coincided with it in Event 2. Allowance for the CME acceleration can change the delay time. According to Gallagher et al. (2003), the maximum CME acceleration in Event 1 was at 0110 UT  $-(+2)$  min, when the front end of the CME had already reached  $0.7R_{\odot}$ . Similar results for Event 2 are not available to us.

Increases in the intensity of relativistic electrons and protons of  $>100$ -MeV had similar time profiles and were observed in the IS from about  $(+25)$  min in both events. This suggests that electrons and protons were accelerated by one of the variants of stochastic acceleration (Petrosyan, 2012; Miller et al., 1997) rather than by shock waves. It should be noted that Kahler (2007), who was confident that protons are accelerated by shock waves, concludes on the same grounds that it is possible to accelerate relativistic electrons by shock waves.

#### 4. DISCUSSION

Flare 1 is an example of SEP events that do not fit into the general statistical patterns of the relationship between proton fluences and  $\mu$ -radiation (Grechnev et al., 2015; Cliver, 2016). According to Cliver (2016), this once again indicates the acceleration of protons by shock waves, not flares. In contrast, Flare 2 corresponds to the statistical patterns (Grechnev et al., 2015).

According to Cliver et al. (2019), the relationship between solar proton events (SPEs) and their parent flare parameters in large, gradual proton events (in the case of a favorable location of the solar flare) can be illustrated by a diagram with three principal parts: (1) the area of the flares caused by the disappearance of the filament and powerful SPEs, (2) the area of a sufficiently high correlation between the parameters of flares and SPEs (main sequence, big-flare syndrome), and (3) the area of medium and large flares that were not accompanied by SPEs. Cliver et al. (2019) believed that the existence of areas (1) and (3) indicates that role of flares in the generation of SPE events is not significant. Flares associated with the disappearance of filament are characterized by weak radio, SXR-, and HXR-emission and low reconnection flux, i.e., flares with an unpronounced impulsive phase. The proton events of April 21 and August 24, 2002, and their parent flares, which are considered in our work, belong to areas (1) and (2), respectively.

Chertok (2018) provides empirical formulas for the estimation of the expected flux of  $>10$  MeV-protons at

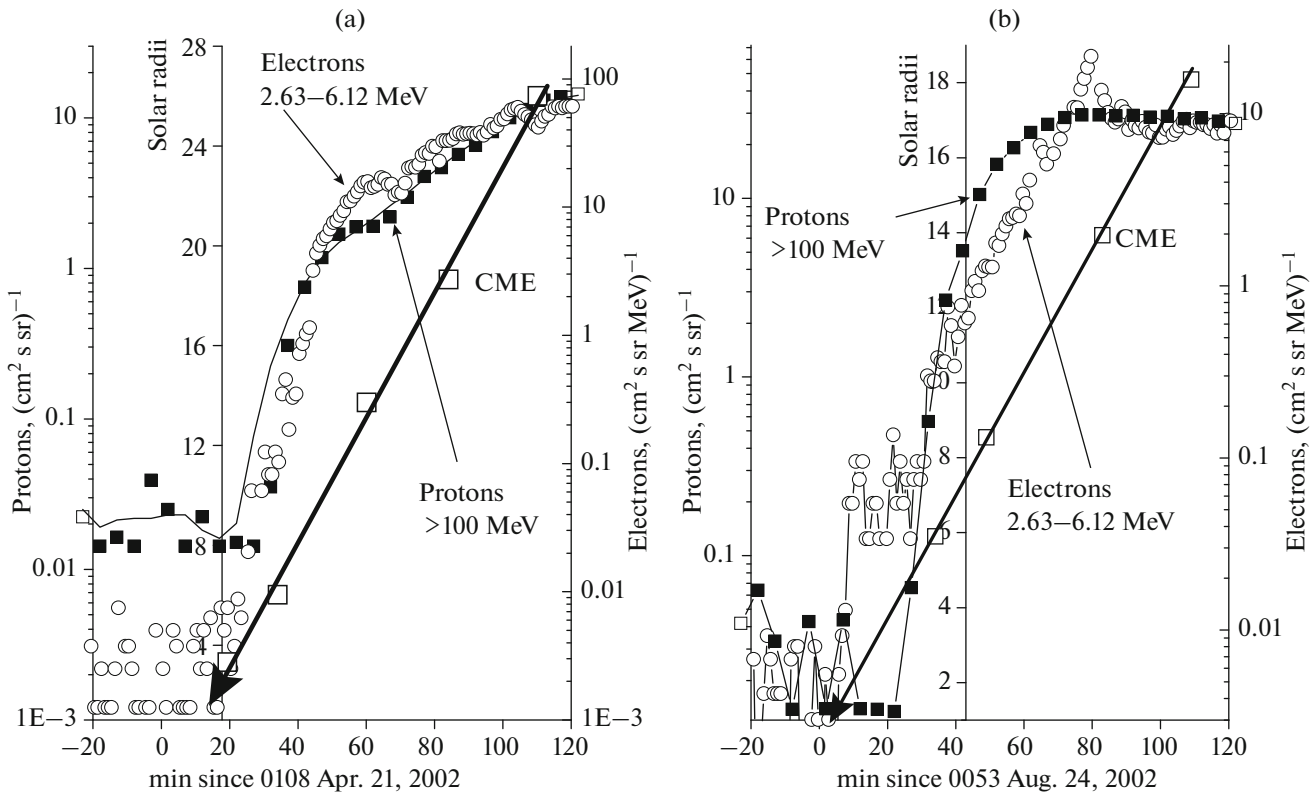


**Fig. 3.** Comparison of the time profiles of >100-MeV proton fluxes (GOES) (black squares) and 2.64- to 6.12-MeV electrons (SOHO EPHIN) (light circles) in the events of (a) Apr. 21, 2002, and (b) Aug. 24, 2002. Approximation of CME position according to the SOHO LASCO data is also shown.

three characteristic frequencies (3000 MHz, 9 GHz, and 15 GHz):

$$\log(J10) = 3.8(\log S3 - 3)^{1.25} + 1.6, \quad S3 > 1000 \text{ sfu},$$

$$\log(J10) = 0.55(\log S9 - 1)^{1.14}, \quad S9 \leq 3000 \text{ sfu},$$

$$\log(J10) = 2.12(\log S9 - 3.5)^{1.729} + 1.56, \quad S9 > 3000 \text{ sfu},$$

$$\log(J10) = 2.24(\log S15 - 3.3)^{1.484} + 1.56, \quad S15 > 2000 \text{ sfu}.$$

Table 3 shows the results of calculations with these formulas for Events 1 and 2. The expected proton flux is about an order of magnitude smaller than the

observed maximum in Event 1 but about an order of magnitude larger than in Event 2. This indicates that the most powerful bursts of radio emission corresponding to short episodes of acceleration in the impulsive phase do not significantly contribute to the maximum proton flux.

In order to achieve large proton fluxes in the scenario given earlier (Struminsky et al., 2020), they must be accelerated and injected into IS for a long time. The total duration of acceleration in pulses corresponding to the pulses of nonthermal radiation is insufficient to accelerate protons to “visible” energies. It may be necessary to use the maximum fluence values rather than the maximum radiation flux values for more accurate predictions (Grechnev et al., 2015). We propose to add the values of the radiation flux by subtracting its pre-

**Table 3.** Maximum fluxes of radio emission, sfu, recorded at three frequencies and estimation of the maximum >10-MeV proton fluxes, sfu, with formulas from Sketch (2018). The last column compares the average calculated proton fluxes with the observed values at maximum intensity

Event	2695 GHz	8.8 GHz	15.4 GHz	Calculated/observed
	sfu/pfu	sfu/pfu	sfu/pfu	pfu/pfu
Apr. 21, 2002	1900/234	2700/32	1300/??	133/2520
Aug. 24, 2002	1200/57	14000/359	17000/3739	1385/317

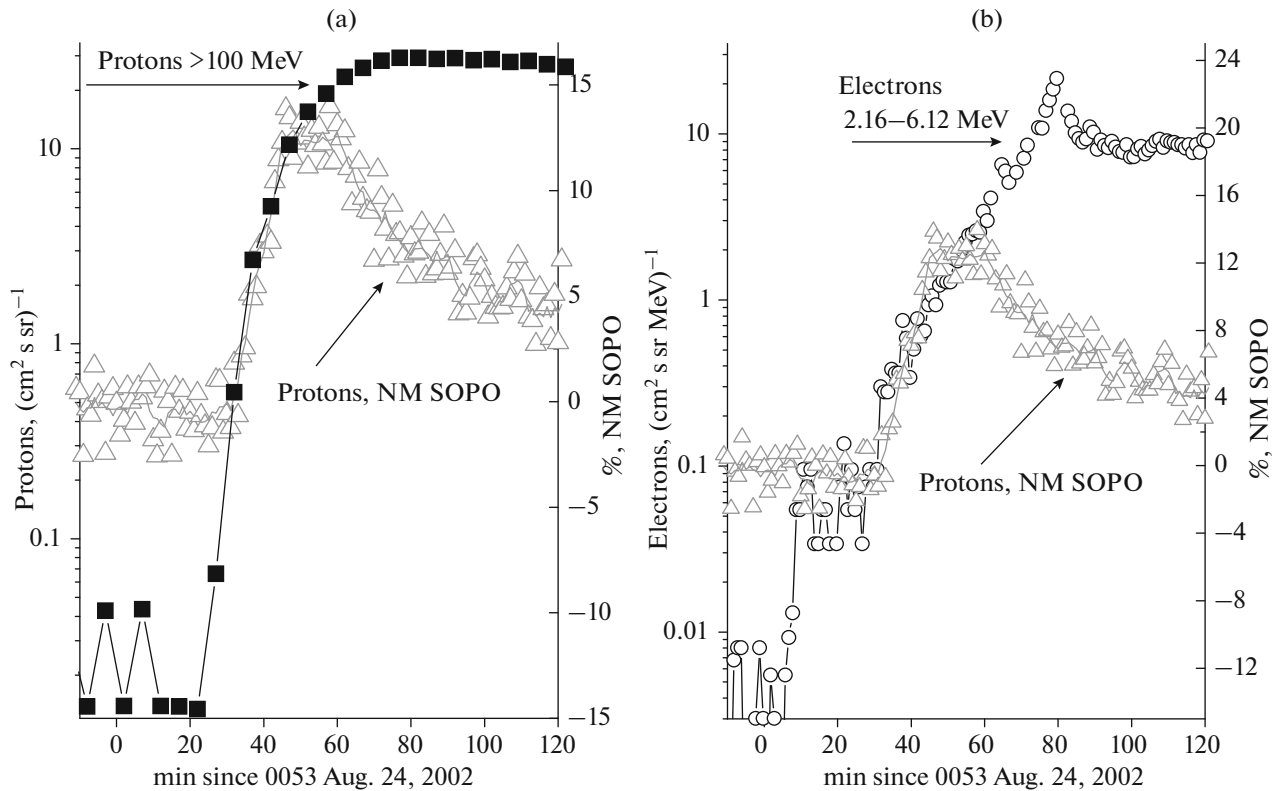


**Fig. 4.** Event of Aug. 24, 2002, comparison of the time profiles of variation (%) of the count rate of South Pole NM (grey triangles) and (a) >100-MeV proton fluxes (GOES) (black squares) and (b) 2.6- to 6.12-MeV electrons (SOHO EPHIN) (light circles).

flare background to calculate the fluxes, in which case the time at which the fluence reaches the plateau will give an effective duration of the process of acceleration of electrons.

Benz (2017) assumed that the flare phenomenon, from an observational point of view, should be defined as an increase in EMR intensity in any energy range from a few minutes to several hours. In our opinion, this definition should be clarified by the fact that EMR is caused by the interaction of energetic particles with matter and magnetic fields of the Sun. With this flare definition, the existence of areas (1) and (3) (Cliver, 2019) will not contradict the role of flares in SPE generation.

Filament eruption and CMEs occur in all gradual flares associated with SPEs (see areas (1) and (2) in (Cliver, 2019)). Filament eruption and CMEs set the characteristic temporal and spatial scale for gradual flares. Flares that are not accompanied by either SPEs or CMEs, area (3) in (Cliver, 2019), are more compact with a duration of less than half an hour and occur in closed magnetic configurations. Such flares are usually associated with processes occurring in the impulsive phase. Apparently, a combination of flares in a particular sequence from areas (1) with a nonpronounced impulsive phase and (3) purely impulsive

phase gives flares from area (2) with a pronounced impulsive phase.

At present, there is no absolutely adequate pattern (scenario) of the initial processes in powerful flares (heating of matter, particle acceleration and their storage and escape into the IS, and the emergence of CMEs and their role in particle acceleration and escape). This article proposes one of the possible scenarios of these processes with an emphasis on the fact that the acceleration of relativistic electrons and protons occurs simultaneously in a large volume of heated matter as a result of long stochastic processes, possibly with multiple and successive reconnections of magnetic structures, which leads to the developed MHD turbulence. After the appearance of the first nonthermal electrons in the solar atmosphere, it should take at least a few minutes before the first protons are detected.

## 5. CONCLUSIONS

The impulsive phase of the flare of April 21, 2002, was not pronounced. (1) The delay in the *EM* maximum relative to the *T* maximum shows that *EM* increased due to an increase in the volume and mass of the emitting plasma (number of loops) rather than its concentration. (2) The intensity of the microwave burst is 15.4 GHz less than that of powerful proton



events. The bursts at other frequencies do not match the proton fluxes observed in the IS. (3) Relativistic electrons were not observed in the IS without protons (at least, the electron flux was smaller than the background one). The situation is opposite in all three items of the list above in the flare with a pronounced impulsive phase that occurred on August 24, 2002.

Increases in the intensity of relativistic electrons and >100-MeV protons had similar time profiles and were observed in the IS starting at (+25) min in both events. This suggests that electrons and protons were accelerated by one of the variants of stochastic acceleration (Petrosyan, 2012; Miller et al., 1997; Struminsky et al., 2020) rather than by shock waves.

The composition of ions accelerated in Flare 2 (Tylka et al., 2005; Tylka et al., 2006), in our opinion, is explained by the rapid and significant evaporation of chromospheric matter in the acceleration region during the impulsive phase.

#### ACKNOWLEDGMENTS

We thank the participants of the ground and space experiments that provided the publicly available data used in this article (GOES, RSTN, RHESSI, SOHO/EPHIN, SOHO/LASCO, and NMDB). We thank the anonymous reviewer for the careful reading of the manuscript and helpful remarks

#### FUNDING

A.B. Struminsky and A.M. Sadovskii acknowledge the support of the project Plasma 2019 and 2020. I.Yu. Grigorieva acknowledges the support of the Energy Release project. Yu.I. Logachev acknowledges the support of Russian Foundation for Basic Research (project no. 19-02-00264).

#### CONFLICT OF INTEREST

The authors declare that they have no conflict of interest.

#### REFERENCES

- Belov, A., Kurt, V., Mavromichalaki, H., and Gerontidou, M., Peak-size distributions of proton fluxes and associated soft X-ray flares, *Sol. Phys.*, 2007, vol. 246, no. 2, pp. 457–470.
- Benz, A.O., Radio spikes and the fragmentation of flare energy release, *Sol. Phys.*, 1985, vol. 96, no. 2, pp. 357–370.
- Benz, A.O., Flare observations, *Living Rev. Sol. Phys.*, 2017, vol. 14, id 2.
- Chertok, I.M., Diagnostic analysis of the solar proton flares of September, 2017, *Geomagn. Aeron. (Engl. Transl.)*, 2018, vol. 58, no. 4, pp. 457–463.
- Cliver, E.W., Flare vs. shock acceleration of high-energy protons in solar energetic particle events, *Astrophys. J.*, 2016, vol. 832, id 128.

- Cliver, E.W., Kahler, S.W., Kazachenko, M., and Shimojo, M., The disappearing solar filament of 2013 September 29 and its large associated proton event: Implications for particle acceleration at the Sun, *Astrophys. J.*, 2019, vol. 877, id 11.
- Daibog, E.I., Melnikov, V.F., and Stolpovskii, V.G., Solar energetic particle events from solar flares with weak impulsive phases of microwave emission, *Sol. Phys.*, 1993, vol. 144, pp. 361–372.
- Gallagher, P.T., Dennis, B.R., and Krucker, S., et al., RHESSI and Trace Observations of the 21 April 2002  $\times 1.5$  flare, *Sol. Phys.*, 2002, vol. 210, no. 1, pp. 341–356.
- Gallagher, P.T., Lawrence, G.R., and Dennis, B.R., Rapid acceleration of a coronal mass ejection in the low corona and implications for propagation, *Astrophys. J.*, 2003, vol. 588, pp. L53–L56.
- Gopalswamy, N., Mäkelä, P., Akiyama, S., et al., Large solar energetic particle events associated with filament eruptions outside of active regions, *Astrophys. J.*, 2015, vol. 806, id 8.
- Grechnev, V.V., Kiselev, V.I., Meshalkina, N.S., and Chertok, I.M., Relations between microwave bursts and near-Earth high-energy proton enhancements and their origin, *Sol. Phys.*, 2015, vol. 290, pp. 2817–2855.
- Grechnev, V.V., Kiselev, V.I., Uralov, A.M., et al., The 26 December 2001 solar eruptive event responsible for GLE63: III. CME, shock waves, and energetic particles, *Sol. Phys.*, 2017, vol. 292, id 102.
- Kahler, S.W., Evidence for solar shock production of heliospheric near-relativistic and relativistic electron events, *Space Sci. Rev.*, 2007, vol. 129, no. 4, pp. 359–390.
- Kocharov, L., Pohjolainen, S., and Mishev, A., et al., Investigating the origins of two extreme solar particle events: Proton source profile and associated electromagnetic emissions, *Astrophys. J.*, 2017, vol. 839, no. 2, id 79.
- Kocharov, L., Pesce-Rollins, M., Laitinen, T., et al., Interplanetary protons versus interacting protons in the 2017 September 10 solar eruptive event, *Astrophys. J.*, 2020, vol. 890, no. 1, id 13.
- Lu, E.T. and Hamilton, R.J., Avalanches and the distribution of solar flares, *Astrophys. J. Lett.*, 1991, vol. 380, no. 2, pp. L89–L92.
- Masson, S., Antiochos, S.K., and DeVore, C.R., Escape of flare-accelerated particles in solar eruptive events, *Astrophys. J.*, 2019, vol. 884, id 143.
- Miller, J.A., Cargill, P.J., and Emslie, A.G., et al., Critical issues for understanding particle acceleration in impulsive solar flares, *J. Geophys. Res.*, 1997, vol. 102, pp. 14631–14660.
- Müller-Mellin, R., Kunow, H., Fleißner, V., et al., COSTEP—Comprehensive suprathermal and energetic particle analyser, *Sol. Phys.*, 1995, vol. 162, nos. 1–2, pp. 483–504.
- Petrosyan, V., Stochastic acceleration by turbulence, *Space Sci. Rev.*, 2012, vol. 73, nos. 1–4, pp. 535–556.
- Ramaty, R., Colgate, S.A., Dulk, G.A., et al., Energetic particles in solar flares, in *Proc. of the 2nd SKYLAB Workshop on Solar Flares*, P.A. Sturrock, Ed., 1978, chap. 4, pp. 117–185.
- Shih, A.Y., Lin, R.P., and Smith, D.M., RHESSI observations of the proportional acceleration of relativistics

- >0.3 MeV electrons and > 30 MeV protons in solar flares, *Astrophys. J.*, 2009, vol. 698, no. 2, pp. L152–L157.
- Struminskii, A.B., Grogor'eva, I.Yu., Logachev, Yu.I., and Sadovsikii, A.M., Solar electrons and protons in the events of September 4–10, 2017 and related phenomena, *Plasma Phys. Rep.*, 2020, vol. 46, no. 2, pp. 176–190.
- Svestka, Z., The phase of particle acceleration in the flare development, *Sol. Phys.*, 1970, vol. 13, no. 2, pp. 471–489.
- Temmer, M., Veronig, A.M., and Kontar, E.P., et al., Combined STEREO/RHESSI study of coronal mass ejection acceleration and particle acceleration in solar flares, *Astrophys. J.*, 2010, vol. 712, no. 2, pp. 1410–1420.
- Tylka, A.J., Cohen, C.M.S., Dietrich, W.F., et al., Shock geometry, seed populations, and the origin of variable elemental composition at high energies in large gradual solar particle events, *Astrophys. J.*, 2005, vol. 625, no. 1, pp. 424–495.
- Tylka, A.J., Cohen, C.M.S., Dietrich, W.F., et al., A comparative study of ion characteristics in the large gradual solar particle events of 2002 April 21 and 2002 August 24, *Astrophys. J. Suppl.*, 2006, vol. 164, no. 2, pp. 536–551.
- Vlahos, L., Particle acceleration in solar flares, *Sol. Phys.*, 1998, vol. 121, nos. 1–2, pp. 431–447.
- Wild, J.P., Smerd, S.F., and Weiss, A.A., Solar bursts, *Ann. Rev. Astron. Astrophys.*, 1963, vol. 1, pp. 291–366.
- Zhang, J., Dere, K.P., and Howard, R.A., et al., On the temporal relationship between coronal mass ejections and flares, *Astrophys. J.*, 2001, vol. 559, no. 1, pp. 452–462.

*Translated by O. Pismenov*